

# Are the maximum shortening velocity and the shape parameter in a Hill-type model of whole muscle related to activation?

M.J. Camilleri<sup>a</sup>, M.L. Hull<sup>a,b,\*</sup>

<sup>a</sup>Biomedical Engineering Program, University of California, Davis, CA 95616, USA

<sup>b</sup>Department of Mechanical Engineering, One Shields Avenue, University of California, Davis, CA 95616, USA

Accepted 30 September 2004

## Abstract

Mathematical models of the inter-relationship of muscle force, velocity, and activation are useful in forward dynamic simulations of human movement tasks. The objective of this work was to determine whether the parameters (maximum shortening velocity  $V_{\max}$  and shape parameter  $k$ ) of a Hill-type muscle model, interrelating muscle force, velocity, and activation, are themselves dependent on the activation. To fulfill this objective, surface EMG signals from four muscles, as well as the kinematics and kinetics of the arm, were recorded from 14 subjects who performed rapid-release elbow extension tasks at 25%, 50%, 75%, and 100% activation (MVC). The experimental elbow flexion angle was tracked by a forward dynamic simulation of the task in which  $V_{\max}$  and  $k$  of the triceps brachii were varied at each activation level to minimize the difference between the simulated and experimental elbow flexion angle. Because a preliminary analysis demonstrated no dependency of  $k$  on activation, additional simulations were performed with constant  $k$  values of 0.15, 0.20, and 0.25. The optimized values of  $V_{\max}$  normalized to the average value within a subject were then regressed onto the activation. Normalized  $V_{\max}$  depended significantly on the activation ( $p < 0.001$ ) for all values of  $k$ . Furthermore, the estimated  $V_{\max}$  values were not sensitive to the selected  $k$  value. The results support the use of Hill-type models in which  $V_{\max}$  depends on activation in forward dynamic simulations modeling muscles with mixed fiber-type composition recruited in the range of 25–100% activation. The use of more accurate models will lend greater confidence to the results of forward dynamic simulations. © 2004 Elsevier Ltd. All rights reserved.

**Keywords:** Muscle; Triceps brachii; Velocity; Concentric; Hill parameter; Contraction; Scaling; Activation

## 1. Introduction

Forward dynamic simulation of human movement provides a powerful tool for both researchers and clinicians to better understand musculoskeletal loading, muscle coordination strategies, and the optimization of human movement activities. In the case of a tracking simulation, the forward simulation progresses so that experimental data, such as measured joint kinematics and kinetics, are tracked by the simulated kinematics and kinetics. In the case of an open-ended simulation, a

task goal, such as maximum jump height, is specified and the simulation progresses to achieve that goal. In both tracking and open-ended simulations, the output includes quantities such as neuromuscular excitations and the forces developed by either individual muscles or groups of muscles with similar functional roles. These simulation outputs have been used to estimate muscle and ligament loads for rehabilitation purposes (Li et al., 1998a), to estimate joint loads during specific occupational tasks (Sparto and Parnianpour, 1998), and to determine muscle coordination strategies for various tasks (Neptune et al., 1997; Raasch et al., 1997; Li et al., 1998b; Bobbert and van Zanwijk, 1999; Neptune et al., 2001).

Forward dynamic simulation utilizes distinct sub-models, each representing specific physiologic, metabolic,

\*Corresponding author. Department of Mechanical Engineering, One Shields Avenue, University of California, Davis, CA 95616, USA. Tel.: +1-530 752 0580; fax: +1-530 752 4158.

E-mail address: mlhull@ucdavis.edu (M.L. Hull).

or anatomic aspects, which are incorporated to produce the simulation results. For example, neural input to the muscles is generally modeled as a first-order differential equation relating the muscle excitation to the activation (Zajac, 1989). Muscle force is then generated as a function of several variables, including muscle activation, length, velocity, fiber-type composition, and activation history (Hill, 1938; Hatze, 1977; Zahalak, 1981; Winters and Stark, 1987; Hatze, 1990; Zahalak and Ma, 1990; Forcinito et al., 1998; Wu and Herzog, 1999). In particular, a Hill-type muscle sub-model is often used to interrelate muscle force and velocity due to its computational efficiency and efficacy in simulating human movement (Raasch et al., 1997; Neptune and Hull, 1998). Muscle forces are transmitted to the skeleton, itself generally represented as a linked chain of rigid bodies (Brand et al., 1982), by means of a 1st order muscle-tendon model (Zajac, 1989). Ultimately, the skeleton and associated limbs respond to these internal loads and other external loads to generate a simulation. The accuracy of this simulation is predicated on the accuracy of each of the sub-models.

While the Hill-type muscle sub-model is well characterized at maximal activation, less is known regarding the effects of submaximal activation on the relationship between muscle force and muscle velocity. Previous *in vivo* experiments (Zahalak et al., 1976) defined activation as a function of the EMG signal; thus activation in part was dependent on the muscle velocity (Basmajian and De Luca, 1985). These results are therefore difficult to apply to current simulation techniques that consider activation and muscle velocity independently. *In vitro* electrical stimulation also has been performed to estimate the interrelationship of muscle activation, force, and velocity (Phillips and Petrofsky, 1980; Durfee and Palmer, 1994) but artificial stimulation does not replicate the natural stereotyped recruitment order, from small to large diameter muscle fibers with increasing excitation (Henneman et al., 1965). Perreault et al. (2003) found that the error associated with a Hill-type muscle equation in feline soleus increased with decreasing stimulation rate, and suggested that this could be explained if the force–velocity properties change with activation. Finally, *in vivo* studies have been performed that investigated the relationship between joint actuator torque and joint actuator angular velocity and activation (Hawkins and Smeulders, 1998; Chow and Darling, 1999); these studies group the linear actuators (muscles) into an angular actuator (torque generator) and appropriately express the velocity as an angular velocity. While these studies relate a generalized load to a generalized speed such as in muscle level studies of force and velocity, the results from these angular motion studies cannot be utilized in forward simulations that implement individual muscle models, which describe linear rather than angular motions.

The development of such a model should consider two sets of findings that relate muscle force–velocity properties to the activation. The first set of findings concern the viscous drag of the myofilaments. Because viscous drag is important in the contractile process (Bagni et al., 1998), the maximum velocity is expected to decrease with decreasing force or activation which is supported by the results of Perreault et al. (2003).

The second set of findings to consider concern the fiber-type ratios and properties in whole muscle. Whole muscle is comprised of muscle fibers of different diameters and muscle fibers with increasingly larger diameters are recruited with increasing activation (Henneman et al., 1965). Additionally, muscle fibers with larger diameters demonstrate larger values of two parameters defining a Hill-type muscle model, the maximum velocity at zero force ( $V_{\max}$ ) and the shape parameter ( $k$ ), the parameter defining the curvature of the force–velocity relationship (Edgerton et al., 1983; Winters and Stark, 1988). Because muscle fibers with different diameters, and hence values of these parameters, will be recruited at any given activation, the whole muscle values of  $V_{\max}$  and  $k$  should represent a composite (weighted average) of the individual parameter values of the active muscle fibers. At low activation, the whole muscle parameter values are expected to resemble the parameter values of small diameter fibers (the first fibers to be activated), whereas at high activation the whole muscle parameter values are expected to shift higher towards those values of larger diameter fibers. Thus, the objective of this study was to test the hypothesis that the parameters ( $V_{\max}$  and  $k$ ) of a Hill-type muscle model, interrelating muscle force, velocity, and activation, are themselves dependent on the activation.

## 2. Methods

To determine whether the values of  $V_{\max}$  and  $k$  depend on the activation, kinematic, kinetic, and EMG data were collected as fourteen subjects performed rapid-release experiments at the elbow joint. The subjects, whose personal data are presented in Table 1, were recruited from the University community and each gave written informed consent. The data acquisition system and experimental apparatus diagrammed in Fig. 1 consisted of an exercise ergometer, an electromagnetic rapid-release mechanism, an electrogoniometer, a wrist brace, four surface EMG electrodes, a data acquisition computer with an analog-to-digital converter, and custom data acquisition software written with LabVIEW (National Instruments, Austin, TX). A steel disk (armature) was attached to a measured location on the wrist brace (proximal to the wrist) at one end and magnetically coupled to the electromagnet at the other

Table 1

Summary of test subject statistics. Average (std. dev.) of age, height, and weight and number of subjects with dominant right hand (left hand)

Sex	Age (years)	Height (m)	Weight (kg)	Dominant hand
Male	28.1 (3.1)	1.77 (0.06)	79.1 (8.3)	10 (1)
Female	25.3 (2.3)	1.75 (0.05)	68.8 (10.5)	3 (0)

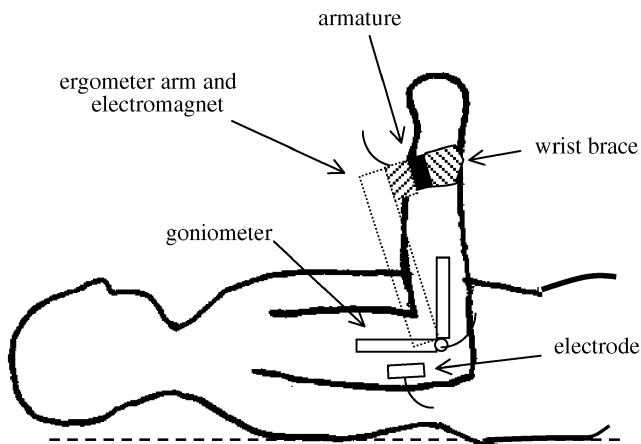


Fig. 1. Diagram of experimental apparatus. Ergometer bench and arm are shown dashed. The ergometer arm, used as a torque-measuring device, was precluded from rotating.

end. The electromagnet was mechanically fixed to the ergometer (Cybex 6000, Computer Sports Medicine, Norwood, MA). The electrogoniometer was taped over the lateral aspect of the subject's elbow on the dominant arm and aligned with the lateral humeral epicondyle. Dominance was defined as the arm naturally used when turning a wrench. Bipolar surface electrodes (Motion-Lab Systems, Baton Rouge, LA) were placed on the shaved and cleaned skin over the motor endplate (Delagi and Perotto, 1980) of each of the triceps brachii and the biceps brachii.

The subjects laid supine at the ergometer, with anatomical joint positions controlled prior to the rapid release experiments. The shoulder was at  $0^\circ$  flexion while the elbow was at  $95^\circ$  flexion (full extension =  $0^\circ$ ). The wrist was at  $0^\circ$  flexion and the forearm was in the neutral position with respect to pronation/supination. The chest and upper arm were strapped to the ergometer.

The maximum elbow torque was determined prior to performing any data collection on the rapid-release experiments. Three trials of maximum voluntary effort isometric elbow extension were performed with a minimum of 2 min between trials. The maximum elbow torque was defined as the average torque of these three trials and activation was defined as the elbow torque divided by the maximum elbow torque.

Each subject performed the rapid-release experiment for three trials each at four activations. The trials were performed in a random order with a minimum of 2 min between trials. The activation was displayed in real time so that the subjects could develop the target activation. To ensure that the activation was at the target value for each trial, current to the electromagnet was terminated only if the actual activation was within  $\pm 5\%$  of the target activation during the preceding 1 s. After terminating current to the electromagnet, kinematic data were collected by means of the electrogoniometer as the elbow extended.

Data used in the analyses were collected during the 1 s prior to rapid release and 40 ms after rapid release. The torque data prior to rapid release was sampled at 1000 Hz and averaged over this period to compute the isometric torque. The electrogoniometer data were sampled at 1000 Hz. The EMG data were sampled at 1000 Hz and band-pass filtered with a low-pass cutoff of 450 Hz and a high-pass cutoff of 5 Hz. Because reflex activity would change the activation, the EMG data were used to confirm that reflex activity in all of the muscles did not occur prior to 40 ms after rapid release. The onset of reflex activity was defined to occur when the EMG activity increased to greater than three standard deviations of the baseline EMG activity (Bedingham and Tatton, 1984). The raw data for each trial were processed as discussed above and then averaged across the three trials for each treatment and subject.

For each subject at each activation, the values of the two parameters ( $V_{\max}$ ,  $k$ ) specifying the force–velocity relationship for the triceps brachii were determined by solving the tracking problem which minimized the error between simulated and experimental elbow flexion angle. The experimental elbow flexion angle ( $\bar{A}$ ) was computed every 1 ms for 40 ms after rapid release by using the electrogoniometer data for each activation and for each subject.

Before performing the forward simulations, the Hill-type equation relating muscle force and velocity was modified to a form commonly used in forward simulations. The Hill-type equation is often presented as

$$(F + a)(V + b) = b(F_{\text{iso}} + a), \quad (1)$$

where  $F$  is the muscle force,  $V$  the muscle velocity,  $F_{\text{iso}}$  the isometric muscle force, and  $a$  and  $b$  are constants. The Hill-type equation was modified algebraically by defining  $k = a/F_{\text{iso}}$  and  $V_{\max} = bF_{\text{iso}}/a$ , where  $k$  is the shape parameter and  $V_{\max}$  is the maximum shortening velocity when  $F$  equals zero. Substituting  $k$  and  $V_{\max}$  into Eq. (1) and solving for  $F$  yields the modified version of the Hill-type equation:

$$F = \frac{F_{\text{iso}}kV_{\max} - F_{\text{iso}}kV}{V + kV_{\max}}. \quad (2)$$

The simulated elbow flexion angle ( $\hat{\theta}$ ) was determined using a forward dynamic model that implemented the modified version of a Hill-type equation for the triceps brachii allowing the muscle parameter values to vary depending on the activation. The force of each individual muscle was determined from Eq. (3):

$$F = \frac{F_{\text{iso}}(a, l)k(a)V_{\text{max}}(a) - F_{\text{iso}}(a, l)k(a)V}{V + k(a)V_{\text{max}}(a)}, \quad (3)$$

where  $F$  is the muscle force,  $V$  the muscle velocity,  $F_{\text{iso}}(a, l)$  the isometric muscle force at activation  $a$  and length  $l$ ,  $V_{\text{max}}(a)$  the maximum shortening velocity of muscle at activation  $a$ , and  $k(a)$  the shape parameter value at activation  $a$  (the determination of the values of  $V_{\text{max}}(a)$  and  $k(a)$  will be discussed shortly). The values of  $F_{\text{iso}}$  for each of the heads of the triceps brachii were computed by equating the triceps tendon force determined by the moment arm and experimental joint torque to the sum of the three muscle forces. Force was distributed to each of the three muscles using muscle force ratio constraints based on the PCSAs of the heads of the triceps taken from the literature (Amis et al., 1979; Murray, 1997). Muscle force was linearly scaled down based on the muscle length and activation (Zajac, 1989). Muscle length was computed by combining (1) knowledge of a reference muscle length at a reference elbow flexion angle (Murray et al., 2000), (2) tendon elongation, and (3) regression equations of triceps brachii tendon moment arm as a function of the elbow flexion angle (Murray, 1997).

$$\text{muscle length} = \int_{\theta_{\text{ref}}}^{\theta} \theta \text{ma}(\theta) d\theta + \text{muscle length}_{\text{ref}} - \text{tendon elongation}, \quad (4)$$

where  $\theta$  is the elbow flexion angle,  $\text{ma}(\theta)$  the moment arm regression equation,  $\theta_{\text{ref}}$  the reference elbow flexion angle, and  $\text{muscle length}_{\text{ref}}$  the reference muscle length. The optimal muscle lengths were estimated based on the work of Murray et al. (2000). Tendon elongation was estimated using a root finding algorithm that matched the muscle force to the tendon force computed using the tendon slack length (Murray et al., 2000) and tendon material properties (Zajac, 1989).

The simulated experimental intersegmental moment ( $\hat{M}$ ) was determined at each time step corresponding to the times at which the experimental elbow flexion angle was computed using the relationship:

$$\hat{M} = \text{triceps moment arm} \times \sum_{i=1}^m F_i, \quad (5)$$

where  $m$  is the number of muscles ( $m=3$ ).

The simulated elbow flexion angle was computed by integrating (fourth-order Runge–Kutta method) the equation of motion ( $\Sigma \text{moments} = \text{moment of iner-$

tia  $\times$  angular acceleration) for 40 ms after rapid release. The equation of motion were generated based on a subject-specific rigid body model using anthropometric data estimated from each subject as well as the inertial properties of the forearm devices. The rigid body model consisted of the moment of inertia of the forearm, hand, and devices, the forearm–hand mass, and the distance of the center of mass of the forearm–hand to the elbow joint axis. The anthropometric data were estimated using scaling factors (de Leva, 1996) while the inertial properties of the forearm devices were computed using knowledge of the device geometry and material properties. Initial conditions for the simulation were the experimental torque and elbow flexion angle at release.

The parameter values ( $V_{\text{max}}$  and  $k$ ) at each activation for each subject were determined by solving a tracking problem. An initial guess of the parameter values was made, and  $\hat{\theta}$  was calculated at each time step of the motion. The parameter values at each activation for each subject were determined by minimizing the objective function  $J_1$  given by

$$J_1 = \sum_{p=1}^n (\theta_p - \hat{\theta}_p)^2, \quad (6)$$

where  $n$  = number of time steps in the simulation ( $n=41$ ). The optimization routine used was a simulated annealing algorithm (Goffe et al., 1994), which has been shown to avoid local minima and converge more rapidly than other optimization methods used in forward dynamic simulations (Neptune, 1999).

The optimized parameter values were normalized on a per subject basis for the statistical analyses. For each subject the value of  $V_{\text{max}}(a)$  was divided by the average of all four  $V_{\text{max}}(a)$  values to yield  $\tilde{V}_{\text{max}}(a)$ , the normalized maximum shortening velocity at activation  $a$ . Similarly,  $k(a)$  was divided by the average of all four  $k(a)$  values to yield  $\tilde{k}(a)$ , the normalized shape parameter at activation  $a$ . The value of  $k$  was constrained between 0.15 and 0.25 (Winters and Stark, 1988).

The functions for  $\tilde{k}$  and  $\tilde{V}_{\text{max}}$  of activation were determined by regression analysis by grouping the data across subjects, using first-order regression models (independent variable was  $a$ , dependent variables were  $\tilde{k}$  and  $\tilde{V}_{\text{max}}$ ). The null hypotheses that  $\tilde{k}$  and  $\tilde{V}_{\text{max}}$  were independent of activation were rejected if the coefficients of the linear terms of the regression equations were significantly different from zero at  $\alpha=0.05$ .

Based on the regression results, the optimized  $k$  values were placed into either one of two categories ( $k=0.15$  or  $0.25$ ) and the frequency within each category was counted. This count indicated that the optimized  $k$  values were equally distributed at the lower (0.15) and upper (0.25) bounds for each activation thus demonstrating that the value of  $k$  was independent of activation. Therefore, three additional sets of simulations

were performed to determine the regression equations relating  $\tilde{V}_{max}$  to activation with  $k$  values of 0.15, 0.20, and 0.25. The regression equations were used to investigate the sensitivity of  $\tilde{V}_{max}$  to  $k$  by computing the maximum variation in  $\tilde{V}_{max}$  at each activation level for the different values of  $k$ .

### 3. Results

Typical kinetic data for the rapid-release experiments demonstrate the consistency of the tests (Fig. 2). The intersegmental elbow moments prior to rapid release, as measured by the ergometer moments, for submaximal activations were within 5% of the target values due to the control software. While it was not possible to precisely control the intersegmental elbow moment at maximum activation, the intersegmental elbow moments for the maximal activations were generally within 5% of each other as well.

Experimental kinematic data demonstrate similar consistency and specific trends between activations (Fig. 3). Isometric elbow flexion angles varied within 3° for each activation, and the angle-time profiles were similar for each activation as well. Post rapid-release elbow flexion angles decreased at faster rates with higher activations, indicative of the greater accelerations and intersegmental elbow moments at higher activations. The elbow flexion angle prior to rapid release progressively decreased with higher activations due to ergometer and subject compliance.

Simulated kinematic data matched well to the experimental kinematic data (Fig. 4). The simulations tracked the experimental data best, over a discrete interval, immediately after rapid release because the initial conditions of the simulation were the experimental conditions at rapid release. As the movement progressed the difference over a discrete interval

typically increased. The simulated elbow flexion angle tracked the experimental elbow flexion angle with an average root mean squared difference of less than 1°.

Typical simulated force–velocity curves resulting from the parameter optimization procedure indicated that isometric force decreased with activation by definition

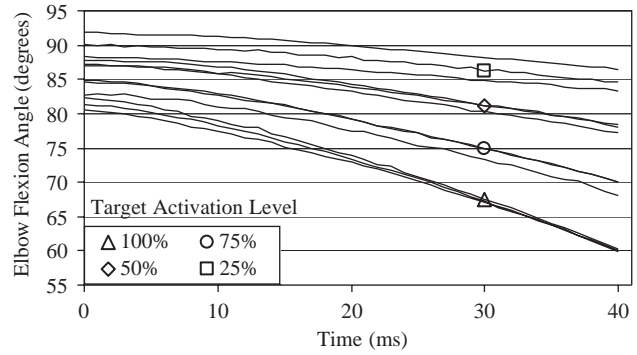


Fig. 3. Example elbow joint angles before and after rapid release for three trials for each of four activation levels for Subject 1. Compliance in the ergometer and subject caused elbow flexion angles prior to rapid release to decrease with increased activation level.

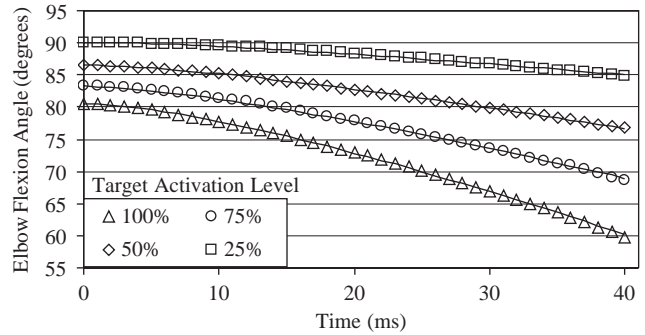


Fig. 4. Example experimental and simulated elbow flexion angles for all four activation levels for Subject 1. Open data points represent experimental elbow flexion angles and solid lines represent simulated elbow flexion angles.

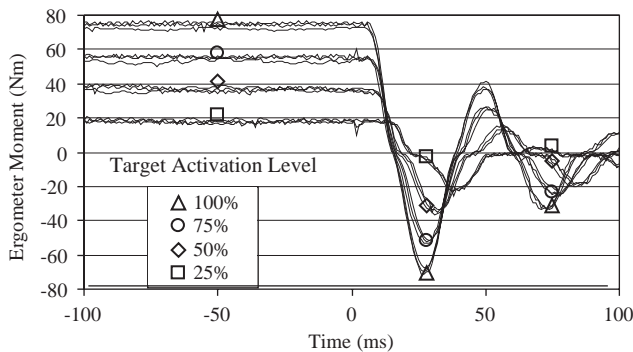


Fig. 2. Example ergometer moments before and after rapid release for three trials for each of four activation levels for Subject 1. Initial flat regions represent the isometric intersegmental elbow moments, whereas the damped oscillations represent the ergometer arm recoiling after uncoupling from the subject.

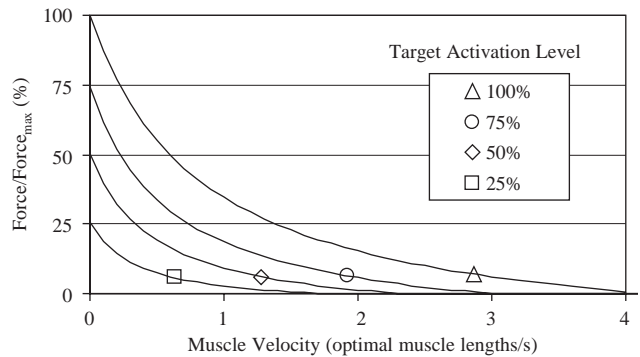


Fig. 5. Simulated force–velocity curves for Subject 1. Activation level markers indicate the maximum velocity attained in the experiment (at 40 ms after rapid release).

Table 2

Summary of the intercepts, slopes, and  $R^2$  values in the regression models relating  $\tilde{V}_{\max}$  to the % activation for different values of  $k$

Statistic	Values of $k$			
	$0.15 \leq k \leq 0.25$	$k = 0.15$	$k = 0.20$	$k = 0.25$
Intercept ( $p$ )	0.506 (<0.0001)	0.448 (<0.0001)	0.448 (<0.0001)	0.397 (<0.0001)
Slope ( $p$ )	0.0080 (<0.0001)	0.0082 (<0.0001)	0.0082 (<0.0001)	0.0090 (<0.0001)
$R^2$	0.66	0.57	0.58	0.64

(Fig. 5).  $V_{\max}$  demonstrated a visual decrease with decreasing activation.

When the normalized maximum shortening velocity  $\tilde{V}_{\max}$  was grouped across subjects, it demonstrated a significant dependence ( $p < 0.001$ ) on the activation for all values of  $k$  (Table 2). The simulated  $\tilde{V}_{\max}$  values were not sensitive to the selected  $k$  value. For example at any activation,  $\tilde{V}_{\max}$  varied at most by 4.7% relative to the  $\tilde{V}_{\max}$  value for  $k = 0.20$  at the same activation. The regression slopes and intercepts indicated that  $\tilde{V}_{\max}$  varied by approximately 46% relative to  $\tilde{V}_{\max}$  at 100% activation over the activations tested.

#### 4. Discussion

Because forward dynamic simulations of movement tasks provide insight into the muscle control strategies and loading of musculoskeletal structures during these tasks and because the mathematical muscle models that are utilized within these simulations are not well characterized at submaximal activation in vivo, the objective of this study was to characterize a Hill-type muscle model at submaximal activation in vivo. Three important findings were that (1) the maximum shortening velocity of muscle depended on the activation, (2) the value of the shape parameter (i.e.  $k$ ) did not depend on the activation, and (3) the maximum shortening velocity was insensitive to the value of  $k$ . However, before discussing the importance of these findings, several methodological issues should be reviewed.

##### 4.1. Methodological issues

In the computation of experimental intersegmental elbow moments and forward dynamic simulations, antagonist muscle activity was not considered which was justified. Pilot tests for this study indicated that typical antagonist (biceps brachii and brachioradialis) EMG activity normalized to the EMG activity elicited during a maximum voluntary isometric elbow flexion task at 90° of flexion was 6%. Moreover, testing in this study was performed such that the extensor fiber lengths were in the plateau region of the force–length curve where force generating capacity is maximum while the

elbow flexor (biceps brachii, brachioradialis, brachialis, and pronator teres) fiber lengths were in the ascending region of the force–length curve (Murray et al., 2000) where force generating capacity is below maximum. Accordingly, the effect of muscle length on muscle force in this study was to decrease the maximum possible effects of the flexors from 10 (brachialis) to 50% (biceps brachii) due to scaling with the force–length curve. Also, joint range of motion was such that the average moment arm for the elbow flexors ranged from 40% less (pronator teres) to 170% more (brachioradialis) than the extensor moment arm (Murray et al., 2000). The PCSA of the elbow flexors is approximately 3% less than that of the elbow extensors (Murray et al., 2000). The combined effects of EMG activity, moment arm length, PCSA ratio, and muscle fiber length are such that the flexors contributed approximately 5% of the total intersegmental elbow moment, which was minimal.

Several possible effects of inaccurate muscle length on the simulation results were analyzed. The error generated from an inaccurate estimate of optimal muscle length was minimized because the rapid-release experiments were conducted such that the muscle lengths were on the plateau region of the force–length curve (Murray et al., 1995). Also, the range of muscle lengths were such that the pennation angle was always less than 15°, which had relatively unimportant effects on muscle-tendon kinematics (Zajac, 1989; Scott and Winter, 1991). Finally, although the shape of the length-tension relationship has been shown to change with activation (Guimaraes et al., 1994), the agonists operated in the plateau region of their force–length curves in this experiment, where the force–activation relationship is relatively insensitive to length (Guimaraes et al., 1994).

To reduce inter-subject variability in the data,  $V_{\max}$  was normalized prior to the regression analysis. Because  $V_{\max}$  depends in part on the muscle length (Lieber, 1992) and because muscle lengths are expected to vary between subjects based on anthropometry,  $V_{\max}$  was expected to differ between subjects, regardless of any other factor.  $V_{\max}$  may also depend on the fiber type compositions of the muscles (Winters and Stark, 1988), which may have differed between subjects. Normalizing each subject's  $V_{\max}$  values thus allowed the data to be pooled across subjects for the regression analysis.

Lastly, because the PCSA ratios used in the model were taken from the literature, a sensitivity analysis was performed to determine the sensitivity of  $\tilde{V}_{\max}$  to changes in the triceps brachii PCSA ratios. Three additional sets of simulations were performed. In each set the relative PCSA of one head of the triceps brachii to the other two was increased by 5%. Forward dynamic simulations were then performed as described previously to determine the values of  $\tilde{V}_{\max}$  at each activation using these new PCSA ratios. Because the values of  $\tilde{V}_{\max}$  changed at most by 0.51% with the new PCSA ratios, the sensitivity of  $\tilde{V}_{\max}$  to the PCSA ratio was small.

4.2. Importance and interpretation of results

The most important finding of our study is that  $V_{\max}$  depends on the activation. As a consequence, muscle models that allow  $V_{\max}$  to vary with activation may yield considerably different muscle forces and activations than models utilizing a constant  $V_{\max}$ . At muscle velocities equal to half the  $V_{\max}$  value the muscle force may be over-estimated in constant  $V_{\max}$  simulations by as much as 170%, 110%, and 60% at activations of 25%, 50%, and 75%, respectively (Fig. 6). To determine the effect of a constant  $V_{\max}$  assumption on the simulated activation within a tracking problem, the experimental elbow flexion angle from the rapid-release tasks at the 25%, 50%, and 75% activations was tracked by using the  $V_{\max}$  value simulated at 100% activation and optimizing the activation. The optimized activations were 17%, 34%, and 57%, or approximately 30% less than the actual activations. These differences are large enough so that conclusions drawn using either the muscle activations or forces derived from forward dynamic simulations may differ depending on whether or not  $V_{\max}$  is allowed to vary with activation.

The variability in our data is comparable to that from previously reported studies. This study determined  $V_{\max}$

at the whole muscle level and this parameter had an average coefficient of variation of 40% at each activation level. At a more detailed level, the  $V_{\max}$  values for muscle fibers, discriminated by fiber-type, had coefficients of variation of approximately 30% (Krivickas et al., 2001). At a grosser level, muscle group parameters had coefficients of variation in the range of 20–45% (Hawkins and Smeulders, 1998; Chow and Darling, 1999). Thus,  $V_{\max}$  determined at all levels ranging from the more detailed fiber level to the more gross muscle group level exhibit comparable levels of variability.

The magnitudes of  $V_{\max}$  determined in this study are also comparable to that determined in other studies (Table 3). Harridge et al. (1996) studied triceps brachii muscle fibers in vitro and found that  $V_{\max}$  (fiber-lengths/s) of the slowest fibers was approximately 8 times less than the smallest  $V_{\max}$  in this study (at 25% activation). While this is a considerable difference, the comparison is appropriately qualified in two respects. The first respect regards the minimum activation in this study. The trend of data (Table 3) suggests activations less than 25% would generate lower  $V_{\max}$  values. The second respect regards the studied quantities. Harridge et al. studied single fibers, whereas this analysis studied whole muscle. It is possible that a range of fiber types were activated even at 25% activation, thus generating a  $V_{\max}$  value representative of both slow and fast-fiber  $V_{\max}$  values. In fact at 100% activation in which all fiber types are activated, the  $V_{\max}$  values computed in this study are less than three times as large as those reported by Harridge et al.

Other important findings of our study are that the Hill parameter  $k$  does not depend on the activation and that the maximum velocity is insensitive to the value of  $k$ . Nevertheless, a value of  $k$  must still be specified in a muscle model used in a forward dynamic simulation. To investigate the sensitivity of force–velocity curves to the  $k$  value, the force–velocity curves resulting from a  $k$  ranging between 0.15 and 0.25 were determined (Fig. 6). For example, at muscle velocities equal to half the  $V_{\max}$

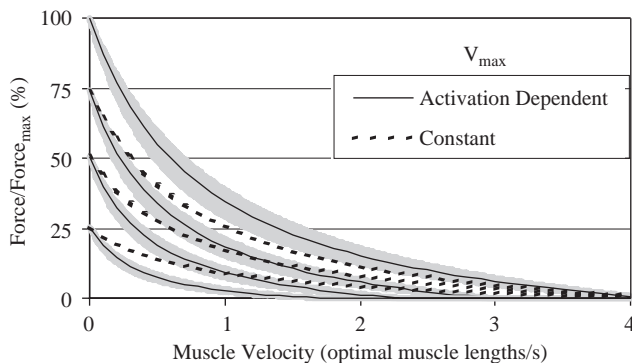


Fig. 6. Simulated force–velocity curves for Subject 1 with activation-dependent  $V_{\max}$  and constant  $V_{\max}$  with  $k=0.20$ . The constant  $V_{\max}$  value was the value at maximum activation (Force/Force<sub>max</sub> = 100%). Grayed areas represent the range of force–velocity curves with  $0.15 \leq k \leq 0.25$ .

Table 3  
 $V_{\max}$  values for the % activations in this study compared with  $V_{\max}$  values for 100% activation from other studies

Author	Muscle	$V_{\max}$ value (std. dev.)
Camilleri and Hull (present article)	Triceps Brachii	3.27 (1.23) 25% activation
		3.64 (1.95) 50% activation
		4.40 (1.59) 75% activation
		5.97 (2.30) 100% activation
Krivickas et al. (2001)	Vastus Lateralis	0.77 (0.22)–2.14 (0.81)
Harridge et al. (1996)	Triceps Brachii	0.27 (0.14)–1.69 (range)
		1.22–2.15)
Fitts et al. (1989)	Deltoid	0.86 (0.04)–4.85 (0.50)

$V_{\max}$  is expressed in optimal muscle-lengths per second for Camilleri and Hull and optimal fiber-lengths per second for all others.

value, the muscle force computed with  $k=0.15$  may be as much as 31% less than the force computed with  $k=0.25$ . Thus, we suggest the use of  $k=0.20$  because the force–velocity curves generated from this value lie approximately in the middle of the range of uncertainty thus minimizing errors in simulations. The equation with  $k=0.20$  that relates  $V_{\max}^*$  to percent activation is

$$V_{\max}^* = 0.353 + 0.00647a \quad (7)$$

where  $V_{\max}^*$  is the maximum shortening velocity at percent activation a normalized to the maximum shortening velocity at 100% activation.

In light of the comments above, applying these results more generally to other muscles is appropriate with specific conditions. One condition is that the muscle fiber-type composition must be similar to that in this study. If the fiber-type composition of a different muscle is considerably different than that in this study, then the response of the muscle parameters to activation may differ from that found in this study. Therefore, these results should be applied to muscles, which are similar in both fiber type composition and variability. As demonstrated by muscle biopsies (Johnson et al., 1973; Staron et al., 2000), among the muscles which meet this condition are many of the large limb muscles (e.g. quadriceps femoris, biceps brachii) used in forward simulation studies.

A second condition is that muscles must demonstrate recruitment as the primary method of force modulation. EMG studies have shown that larger, power-producing muscles of the shoulder and elbow primarily demonstrate recruitment, whereas the smaller, accuracy driven muscles of the hand and wrist primarily demonstrate rate-coding (Kukulka and Clamann, 1981; De Luca et al., 1982). While a search of the literature did not reveal any similar studies of muscles of the lower limb, the method of force modulation for the large lower limb muscles is expected to be similar given that the objective of these muscles is similar (i.e. gross force production). Accordingly, these results are important to forward simulation studies that incorporate large limb muscles (e.g. Li et al., 1998a; Bobbert and van Zandwijk, 1999; Neptune and Hull, 1999).

Because this study investigated activations greater than 25%, activations greater than or equal to 25% is a final condition to applying these results more generally. At activations less than this value, rate-coding may be the dominant method of force modulation in large limb muscles (De Luca et al., 1982; Hawkins and Hull, 1992), thus violating the first condition discussed above. This minimum activation value is appropriate for forward simulations of many common tasks, such as jumping (Bobbert and van Zandwijk, 1999), pedaling (Neptune and Hull, 1998), and knee extension exercises (Li et al., 1998a).

In summary, forward dynamic simulation of rapid-release tasks has provided an effective means by which to evaluate the response of  $V_{\max}$  to activation. When data are grouped across subjects,  $V_{\max}$  demonstrates a dependency on the activation within a range of 25–100%. The use of Hill-type muscle models in which  $V_{\max}$  varies with activation can greatly increase the accuracy and confidence of results from forward dynamic simulations.

## References

- Amis, A.A., Dowson, D., Wright, V., 1979. Muscle strengths and musculoskeletal-geometry of the upper limb. *Engineering in Medicine* 8, 41–48.
- Bagni, M.A., Cecchi, G., Cecchini, E., Colombini, B., Colomo, F., 1998. Force responses to fast ramp stretches in stimulated frog skeletal muscle fibres. *Journal of Muscle Research and Cell Motility* 19, 33–42.
- Basmajian, J.V., De Luca, C.J., 1985. *Muscles Alive: Their Functions Revealed by Electromyography*. Williams & Wilkins, Baltimore, MD.
- Bedingham, W., Tatton, W.G., 1984. Dependence of EMG responses evoked by imposed wrist displacements on pre-existing activity in the stretched muscles. *Canadian Journal of Neurological Sciences* 11, 272–280.
- Bobbert, M.F., van Zandwijk, J.P., 1999. Sensitivity of vertical jumping performance to changes in muscle stimulation onset times: a simulation study. *Biological Cybernetics* 81, 101–108.
- Brand, R.A., Crowninshield, R.D., Wittstock, C.E., Pedersen, D.R., Clark, C.R., van Krieken, F.M., 1982. A model of lower extremity muscular anatomy. *Journal of Biomechanical Engineering* 104, 304–310.
- Chow, J.W., Darling, W.G., 1999. The maximum shortening velocity of muscle should be scaled with activation. *Journal of Applied Physiology* 86, 1025–1031.
- de Leva, P., 1996. Adjustments to Zatsiorsky–Seluyanov’s segment inertia parameters. *Journal of Biomechanics* 29, 1223–1230.
- De Luca, C.J., LeFever, R.S., McCue, M.P., Xenakis, A.P., 1982. Behaviour of human motor units in different muscles during linearly varying contractions. *Journal of Physiology* 329, 113–128.
- Delagi, E.F., Perotto, A., 1980. *Anatomic Guide for the Electromyographer—The Limbs*. Thomas, Springfield, IL.
- Durfee, W.K., Palmer, K.I., 1994. Estimation of force-activation, force-length, and force-velocity properties in isolated, electrically stimulated muscle. *IEEE Transactions on Biomedical Engineering* 41, 205–216.
- Edgerton, V.R., Roy, R.R., Bodine, S.C., Sacks, R.D., 1983. The matching of neuronal and muscular physiology. In: Borer, K.T., Edington, D.W., White, T.P. (Eds.), *Frontiers of Exercise Biology*. Human Kinetics Publishers, Champaign, IL., pp. 123–145.
- Fitts, R.H., Costill, D.L., Gardetto, P.R., 1989. Effect of swim exercise training on human muscle fiber function. *Journal of Applied Physiology* 66, 465–475.
- Forcinito, M., Epstein, M., Herzog, W., 1998. Can a rheological muscle model predict force depression/enhancement? *Journal of Biomechanics* 31, 1093–1099.
- Goffe, W.L., Ferrier, G.D., Rogers, J., 1994. Global optimization of statistical functions with simulated annealing. *Journal of Econometrics* 60, 65–99.
- Guimaraes, A.C., Herzog, W., Hulliger, M., Zhang, Y.T., Day, S., 1994. Effects of muscle length on the EMG-force relationship of the cat soleus muscle studied using non-periodic stimulation of ventral root filaments. *Journal of Experimental Biology* 193, 49–64.

- Harridge, S.D., Bottinelli, R., Canepari, M., Pellegrino, M.A., Reggiani, C., Esbjornsson, M., Saltin, B., 1996. Whole-muscle and single-fibre contractile properties and myosin heavy chain isoforms in humans. *European Journal of Physiology* 432, 913–920.
- Hatze, H., 1977. A myocybernetic control model of skeletal muscle. *Biological Cybernetics* 25, 103–119.
- Hatze, H., 1990. The charge transfer model of myofibrillar interaction: prediction of force enhancement and related myodynamic phenomena. In: Woo, S.L.Y., Winters, M.J. (Eds.), *Multiple Muscle Systems: Biomechanics and Movement Organization*. Springer, New York, NY, pp. 24–45.
- Hawkins, D., Smeulders, M., 1998. Relationship between knee joint torque, velocity, and muscle activation: considerations for musculoskeletal modeling. *Journal of Applied Biomechanics* 14, 141–157.
- Hawkins, D.A., Hull, M.L., 1992. An activation-recruitment scheme for use in muscle modeling. *Journal of Biomechanics* 25, 1467–1476.
- Henneman, E., Somjen, G., Carpenter, D.O., 1965. Excitability and inhibibility of motoneurons of different sizes. *Journal of Neurophysiology* 28, 599–620.
- Hill, A., 1938. The heat of shortening and the dynamic constants of muscle. *Proceedings of the Royal Society of London* 126, 136–195.
- Johnson, M.A., Polgar, J., Weightman, D., Appleton, D., 1973. Data on the distribution of fibre types in thirty-six human muscles: an autopsy study. *Journal of the Neurological Sciences* 18, 111–129.
- Krivickas, L.S., Suh, D., Wilkins, J., Hughes, V.A., Roubenoff, R., Frontera, W.R., 2001. Age- and gender-related differences in maximum shortening velocity of skeletal muscle fibers. *American Journal of Physical Medicine and Rehabilitation* 80, 447–455.
- Kukulka, C.G., Clamann, H.P., 1981. Comparison of the recruitment and discharge properties of motor units in human brachial biceps and adductor pollicis during isometric contractions. *Brain Research* 219, 45–55.
- Li, G., Kawamura, K., Barrance, P., Chao, E.Y., Kaufman, K., 1998a. Prediction of muscle recruitment and its effect on joint reaction forces during knee exercises. *Annals of Biomedical Engineering* 26, 725–733.
- Li, Z.M., Latash, M.L., Zatsiorsky, V.M., 1998b. Force sharing among fingers as a model of the redundancy problem. *Experimental Brain Research* 119, 276–286.
- Lieber, R.L., 1992. *Skeletal Muscle Structure and Function: Implications for Rehabilitation and Sports Medicine*. Williams & Wilkins, Baltimore, MD.
- Murray, W.M., 1997. The functional capacity of elbow muscles: anatomical measurements, computer modeling, and anthropometric scaling. Ph.D., Biomedical Engineering, Northwestern University.
- Murray, W.M., Delp, S.L., Buchanan, T.S., 1995. Variation of muscle moment arms with elbow and forearm position. *Journal of Biomechanics* 28, 513–525.
- Murray, W.M., Buchanan, T.S., Delp, S.L., 2000. The isometric functional capacity of muscles that cross the elbow. *Journal of Biomechanics* 33, 943–952.
- Neptune, R.R., 1999. Optimization algorithm performance in determining optimal controls in human movement analyses. *Journal of Biomechanical Engineering* 121, 249–252.
- Neptune, R.R., Hull, M.L., 1998. Evaluation of performance criteria for simulation of submaximal steady-state cycling using a forward dynamic model. *Journal of Biomechanical Engineering* 120, 334–341.
- Neptune, R.R., Hull, M.L., 1999. A theoretical analysis of preferred pedaling rate selection in endurance cycling. *Journal of Biomechanics* 32, 409–415.
- Neptune, R.R., Kautz, S.A., Hull, M.L., 1997. The effect of pedaling rate on coordination in cycling. *Journal of Biomechanics* 30, 1051–1058.
- Neptune, R.R., Kautz, S.A., Zajac, F.E., 2001. Contributions of the individual ankle plantar flexors to support, forward progression and swing initiation during walking. *Journal of Biomechanics* 34, 1387–1398.
- Perreault, E.J., Heckman, C.J., Sandercock, T.G., 2003. Hill muscle model errors during movement are greatest within the physiologically relevant range of motor unit firing rates. *Journal of Biomechanics* 36, 211–218.
- Phillips, C.A., Petrofsky, J.S., 1980. Velocity of contraction of skeletal muscle as a function of activation and fiber composition: a mathematical model. *Journal of Biomechanics* 13, 549–558.
- Raasch, C.C., Zajac, F.E., Ma, B., Levine, W.S., 1997. Muscle coordination of maximum-speed pedaling. *Journal of Biomechanics* 30, 595–602.
- Scott, S.H., Winter, D.A., 1991. A comparison of three muscle pennation assumptions and their effect on isometric and isotonic force. *Journal of Biomechanics* 24, 163–167.
- Sparto, P.J., Parnianpour, M., 1998. Estimation of trunk muscle forces and spinal loads during fatiguing repetitive trunk exertions. *Spine* 23, 2563–2573.
- Staron, R.S., Hagerman, F.C., Hikida, R.S., Murray, T.F., Hostler, D.P., Crill, M.T., Ragg, K.E., Toma, K., 2000. Fiber type composition of the vastus lateralis muscle of young men and women. *Journal of Histochemistry and Cytochemistry* 48, 623–629.
- Winters, J.M., Stark, L., 1987. Muscle models: what is gained and what is lost by varying model complexity. *Biological Cybernetics* 55, 403–420.
- Winters, J.M., Stark, L., 1988. Estimated mechanical properties of synergistic muscles involved in movements of a variety of human joints. *Journal of Biomechanics* 21, 1027–1041.
- Wu, J.Z., Herzog, W., 1999. Modeling concentric contraction of muscle using an improved cross-bridge model. *Journal of Biomechanics* 32, 837–848.
- Zahalak, G.I., 1981. A distribution-moment approximation for kinetic theories of muscular contraction. *Mathematical Biosciences* 55, 89–114.
- Zahalak, G.I., Ma, S.P., 1990. Muscle activation and contraction: constitutive relations based directly on cross-bridge kinetics. *Journal of Biomechanical Engineering* 112, 52–62.
- Zahalak, G.I., Duffy, J., Stewart, P.A., Litchman, H.M., Hawley, R.H., Paslay, P.R., 1976. Partially activated human skeletal muscle; an experimental investigation of force, velocity, and EMG. *Journal of Applied Mechanics* 43, 81–86.
- Zajac, F.E., 1989. Muscle and tendon: properties, models, scaling, and application to biomechanics and motor control. *Critical Reviews in Biomedical Engineering* 17, 359–411.